Evaluating the JULES Land Surface Model Energy Fluxes Using FLUXNET Data

ELEANOR BLYTH

Centre for Ecology and Hydrology, Wallingford, United Kingdom

JOHN GASH

Centre for Ecology and Hydrology, Wallingford, United Kingdom, and VU University, Amsterdam, Netherlands

AMANDA LLOYD

Centre for Ecology and Hydrology, Wallingford, United Kingdom

MATTHEW PRYOR AND GRAHAM P. WEEDON

Met Office Hadley Centre for Climate Prediction and Research (Joint Centre for Hydro-Meteorological Research), Wallingford, United Kingdom

JIM SHUTTLEWORTH

Centre for Ecology and Hydrology, Wallingford, United Kingdom, and Department of Hydrology and Water Resources, The University of Arizona, Tucson, Arizona

(Manuscript received 8 June 2009, in final form 22 October 2009)

ABSTRACT

Surface energy flux measurements from a sample of 10 flux network (FLUXNET) sites selected to represent a range of climate conditions and biome types were used to assess the performance of the Hadley Centre land surface model (Joint U.K. Land Environment Simulator; JULES). Because FLUXNET data are prone systematically to undermeasure surface fluxes, the model was evaluated by its ability to partition incoming radiant energy into evaporation and how such partition varies with atmospheric evaporative demand at annual, seasonal, weekly, and diurnal time scales. The model parameters from the GCM configuration were used. The overall performance was good, although weaknesses in model performance were identified that are associated with the specification of the leaf area index and plant rooting depth, and the representation of soil freezing.

1. Introduction

Evaporation from the land surface is a major component of the global water cycle. The Bowen ratio of land surfaces modulates the thermodynamics and dynamics of atmospheric circulation, which determines surface–climate feedbacks (Lawrence et al. 2007). Evaporation also transfers water from plants and soil to the atmosphere and influences water resources and runoff. Accurate model calculations of evaporation are therefore needed at the global scale to investigate the possible perturbation of the global water cycle resulting from climate change. Land surface models that can make such calculations exist, but their performance requires evaluation against existing data across a range of vegetation types and in different climates.

Historical observations of land surface evaporation are sparse: the Intergovernmental Panel on Climate Change (IPCC) technical report on water and climate (Bates et al. 2008) described evaporation as the weakest link in the water cycle chain. In contrast to rainfall or river runoff, there are no publicly available global evaporation data.

Corresponding author address: Eleanor Blyth, Centre for Ecology and Hydrology, Wallingford OX10 8BB, United Kingdom.
E-mail: emb@ceh.ac.uk

DOI: 10.1175/2009JHM1183.1

However, relevant surface exchange data are becoming available through the flux network (FLUXNET; Baldocchi et al. 2001). Many medium-term (5–10 years), ground-based observations of carbon dioxide and surface energy fluxes are now being made by FLUXNET at a network of locations across the world in different climate zones and over different ecosystems. Therefore, FLUXNET is arguably the most comprehensive terrestrial ecosystem dataset currently available, with more than 400 flux towers operating either independently or as part of regional networks, such as CarboEurope, AmeriFlux, and the Large-Scale Biosphere–Atmosphere Experiment in Amazonia (LBA). The micrometeorological technique used samples over a footprint of a few hundred meters upwind; however, unlike remotely sensed or catchment water balance estimates of evaporation, FLUXNET observations are provided continuously over long periods and at subdaily time scale. Such characteristics are attractive to land surface model developers, and Stöckli et al. (2008), for example, used FLUXNET data to inform development of the Community Land Model (CLM) land surface model.

The earth science community is therefore interested in the potential use of FLUXNET observations as benchmark data to evaluate the performance of the land surface models used in GCMs (Stöckli et al. 2008). This paper describes a pathfinder study whose goal is to determine if and how FLUXNET data can be used in this way. In particular, we address how the performance of the Joint U.K. Land Environment Simulator (JULES; Blyth et al. 2006; Hadley Centre land surface model) merit further development.

Perhaps the most important shortcoming of FLUXNET data is that the time average sum of measured outgoing latent and sensible heat fluxes does not always equal the time average observed incoming radiant energy; that is, that the ''energy closure'' of the eddy covariance systems used by FLUXNET is imperfect (Wilson et al. 2002). The extent of imbalance between the observed incoming and outgoing energy varies between sites and may vary with time and atmospheric conditions at a specific site. This issue was explored recently in a series of experiments under the Energy Balance Experiment (EBEX) framework (Oncley et al. 2007; Mauder et al. 2007). Some of the FLUXNET sites seem to get good closure, whereas others do not; there is no consensus on the reasons. Haverd et al. (2007) and Meyers and Hollinger (2004) have shown that it is possible to account for the storage terms in the models. However, under measurement of energy fluxes is most commonly observed, perhaps because data are for less-than-ideal micrometeorological sites, or because of shortcomings in data sampling and averaging protocols (Finnigan 2004; Finnigan et al. 2003) or errors associated with the physical characteristics of the equipment (e.g., Gash and Dolman 2003; van der Molen et al. 2004).

Following Sellers et al. (1989), the present study assumes that the fractional misbalance of energy outgoing as latent and sensible heat in FLUXNET data is on average the same. Model-calculated evaporation is therefore compared with observed evaporation that has been normalized by the ratio of modeled available energy to the sum of the observed latent and sensible heat. This method was also used by Twine et al. (2000). Consequently, the aspect of JULES performance that is evaluated is the model's ability to partition incoming radiant energy into latent heat and how this partition varies with evaporative demand of the atmosphere for a sample of 10 FLUXNET sites selected across a range of biomes and climates.

The model parameters were not tuned in any way. Instead, parameters for the model were taken as though it were embedded in the GCM, so that default values of soil properties and vegetation properties were taken from the lookup tables used in the operational version of the model. The aim of the paper is to investigate whether the data themselves have value for the land surface model, rather than whether the model can replicate the data. The aspect of the model being tested is its ability to partition the available energy into sensible and latent heat. The observed fluxes of sensible and latent heat are therefore ''normalized'' by the observed available energy (the sum of the observed sensible and latent heat fluxes), thus obviating the need to consider the radiation budget, or storage terms in the soil or the canopy. It is hoped that these data can then be used as a benchmark of the performance of the model in its operational mode.

2. FLUXNET sites

To minimize the possible effect of under measurement of surface energy fluxes at FLUXNET sites for this analysis, sites were selected where mean daily energy closure was within 30%. Selected sites also had a data record with little (less than 20%) gap filling for more than three consecutive years. These limits were chosen because they are not too restrictive on the range of sites that can be used but ensure reasonable data quality. Ten FLUXNET sites that satisfied these requirements were then further selected to sample a range of climate zones (temperate, Mediterranean, tropical, and boreal) and plant functional types and soils. Model forcing was extracted from among the measured variables for each site for all the years that they were available and for the measured fluxes in the year chosen for model evaluation. Gap filling involved, for each precise time step that was missing, using the average of values from other

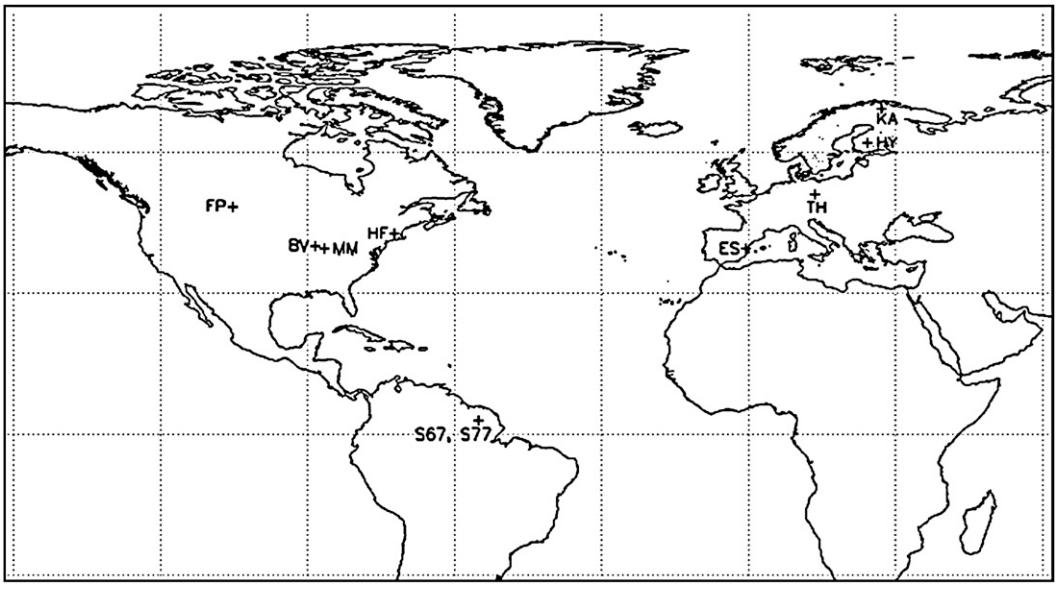

FIG. 1. Location of the FLUXNET sites used in this study labeled as follows: FP = Fort Peck; BV = Bondville; MM = Morgan Monroe; HF = Harvard Forest; S67 = Santarem km 67, Brazil; S77 = Santarem km 77, Brazil; KA = Kaamenen; HY = Hyytiälä; TH = Tharandt; and ES = El Saler.

years at the same time step. This method has the merit of preserving both diurnal and seasonal cycles in the meteorological forcing variables at the expense of some loss in subdiurnal variability.

The locations of the 10 study sites selected are shown in Fig. 1, and the plant functional types and soils specified by FLUXNET and climate for the selected sites are summarized in Table 1. The yearly weather data given in Table 1 are calculated from FLUXNET data for the year in which comparison was made.

Although only 10 sites were considered in this prototype study, the selection does include helpful contrasts. For three of the climate zones considered (boreal, temperate, and tropical), data for at least one pair of contrasting plant functional types (trees and grass) is included. The two Amazonian sites, for example, sample the contrast between forest and logged pasture: an important land use change in the humid tropics. The selected sites also include a north–south European climate transect between Kaamanen and Hyytiälä in Finland, through Tharandt in Germany, to El Saler in southern Spain. Selected sites in the United States are at similar latitude but sample an east–west precipitation gradient, from the dry climate of Fort Peck, Montana, toward wetter regions through Bondville, Illinois, and Morgan Monroe, Indiana, to the Harvard Forest, Massachusetts, in the east. The loamy soils at the Harvard site also contrast with the clay soils at Morgan Monroe.

Because the comparison between observed- and model-calculated surface energy fluxes was made at sites with different climates, it is instructive to characterize the evaporative demand of the atmosphere and its seasonal dependence at the FLUXNET sites. The Priestley–Taylor (P–T) equation (Priestley and Taylor 1972) was adopted for this purpose. The P–T equation assumes the latent heat flux λE transported in the water vapor leaving the evaporating surfaces is

$$\lambda E = \alpha \frac{\Delta A}{\Delta + \gamma}, \tag{1}$$

where A is the energy available at the surface to convert liquid water to water vapor or to warm the overlying air, Δ is the rate of change of saturated vapor pressure with temperature, and γ is the psychrometric constant. With $\alpha = 1$, Eq. (1) calculates equilibrium evaporation—that is, evaporation into air that is always saturated. In the natural world, the air overlying moist evaporating surfaces is rarely saturated and therefore α is greater than unity. Priestley and Taylor (1972) evaluated evaporation data from several sites and on this basis suggested using $\alpha = 1.26$, a value that has subsequently often been adopted. De Bruin (1983) and McNaughton and Spriggs (1989) used a coupled model to explore surface atmosphere feedbacks and suggested that for surface resistances not untypical of a range of vegetation, the value 1.26 does provide an approximate estimate of area-average evaporation in humid climates. Although clearly a higher value would be needed in more arid climates, we are only using the P–E evaporation for scaling. Thus, in this study

TABLE 1. FLUXNET site description and mean meteorological variables.

Site name (year selected for comparison)	Plant functional type	Soil type	LAI (monthly)	Available years of data	Climate zone	Mean temperature (°C)	Annual precipitation (to nearest 10 mm)	Annual average ratio of evaporation to precipitation
KA (2002)	Wetlands (designated grass)	Peat (sand in model)	2	6	Boreal	−1	440	0.50
HY (2000)	Evergreen needleleaf	Sand	4	10	Boreal	5	530	0.59
MM (2002)	Deciduous broadleaf	Clay	(0.2, .2, 0.2, 1, 2, 5, 5, 5, 2, 1, .2, .2)	7	Temperate	13	1150	0.43
HF (1999)	Deciduous broadleaf	Loam	(0.2, .2, 0.2, 1, 2, 5, 5, 5, 2, 1, .2, .2)	13	Temperate	9	1030	0.48
TH (1999)	Evergreen needleleaf	Loam	4	8	Temperate	9	640	0.77
BV (1998)	Cropland, soybean, maize rotation (designated grass with variable LAI)	Loam	(0.2, .2, 0.2, 1, 2, 2, 2, 2, 2, 1, .2, .2)	10	Temperate	13	930	0.68
ES (1999)	Evergreen needleleaf	Sand	4	5	Mediterranean	17	440	0.83
FP (2006)	Grass	Loam	2	7	Mediterranean	7	320	1.0
S67 (2003)	Evergreen needleleaf	Clay	4	3	Tropical	25	1290	0.84
S77 (2003)	Grass	Clay	2	5	Tropical	26	1610	0.56

we adopt $\alpha = 1.26$ in Eq. (1) to provide a measure of the daily average evaporative demand of the atmosphere at the selected FLUXNET sites.

In Eq. (1) the term $\Delta/(\Delta + \gamma)$ varies almost linearly from about 0.4 to about 0.8 as air temperature changes from 0° to 33°C, indicating that air temperature at the FLUXNET site can have a significant influence on atmospheric demand. If the observed time-average evaporation over a day or longer is significantly lower than the estimate given by Eq. (1), it can be assumed that there is insufficient water available at the land surface to meet atmospheric demand.

3. Modeled energy fluxes

Version 2 of the offline land surface model used in the Hadley Centre GCM is referred to as JULES (Blyth et al. 2006). This model was used to calculate the fluxes. JULES is based on the Met Office Surface Exchange System (MOSES) model described by Cox et al. (1999) and includes mechanistic formulations of the physical, biophysical, and biochemical processes that control the radiation, heat, water, and carbon fluxes in response to hourly conditions of the overlying atmosphere. JULES has integrated the coupling of photosynthesis, stomatal conductance, and transpiration so that the biophysical processes in the vegetation interact with hydrological processes in the soil.

In this study, the modeling protocol was to use standard model parameters with no optimization of parameters to enhance local agreement between observed- and model-calculated surface energy fluxes. In general, the model parameters selected for use in the calculations made using JULES at each site were selected to match the vegetation and soil specified for each site (described online at http://www.fluxnet.ornl.gov/fluxnet/siteplan.cfm). Vegetation parameters were specified for a single vegetation type from the standard lookup table used in the Hadley Centre GCM to represent needleleaf trees, broadleaf trees, C3 grassland, and C4 grassland as appropriate; see Table 1. Soil properties were assumed uniform in the vertical dimension. The soils at the FLUXNET sites given in Table 1 were appropriately reclassified into those used in the Hadley Centre GCM; hence, clay became fine soil, loam became medium soil, and sand became coarse soil. Soil parameters corresponding to the fine, medium, and coarse soil classes were then taken from the standard lookup table used by the Hadley Centre GCM. In the case of the Harvard and Morgan Monroe deciduous forest sites and the Bondville crop site, imposing the fixed leaf area index (LAI) normally used in the GCM is unrealistic and gave rise to substantial errors in the modeled fluxes. In these three cases, the magnitude and timing of the annual

cycle in leaf area index given in the FLUXNET data (see Table 1) was therefore imposed.

The gap-filled, multiyear meteorological forcing data measured at the FLUXNET sites were used to drive the JULES model, with the first two years of driving data repeatedly applied to spin up the model from an arbitrary starting point with soil temperature initially set to 283 K and soil moisture to 80% of saturation. After spin up, model-calculated values using the chosen year of driving data were compared with the field observations made in that year.

4. Results

a. Annual and seasonal time scales

The seasonal influences on evaporation differ substantially between the selected sites. Previous studies of boreal forest systems (Harding et al. 2001), for example, indicate strong seasonality in land surface control on evaporation. In winter when the ground is covered in snow and sun angles are low, the forest floor is permanently shaded and the darker forest canopy absorbs almost all the incoming solar radiation, but there can be no transpiration while the soils are frozen. On the other hand, the subsequent high radiation in spring fuels substantial heat fluxes into the atmosphere and ground. In temperate regions, early field campaigns demonstrated the importance of evaporation of intercepted water from forest sites (Stewart 1977). This has been demonstrated in more recent studies (Gerrits et al. 2007; Guevara-Escobar et al. 2007) so that one of the key drivers of evaporation is therefore leaf area index (Blyth 2008), because of both its relation to canopy–surface water storage, and its influence on transpiration. Changes in leaf cover also contribute to distinctly different seasonal evaporation rates for evergreen and deciduous trees and crops compared to grassland. The study of dry and Mediterranean sites motivated field campaigns [e.g., the Hydrologic and Atmospheric Pilot Experiment in the Sahel (HAPEX-Sahel); Goutorbe et al. 1997] that showed that evaporation is strongly controlled by rainfall in climates with hot dry seasons when evaporation is low despite high evaporative demand. Summarizing the results of the Anglo–Brazilian Amazonian Climate Observational Study (ABRACOS), Nobre et al. (1996) stated that Amazonian forest shows little seasonality in surface energy partition because tree roots are deep and water supply consistently plentiful, but re-evaporation of intercepted water remains important as it is for temperate forests. On the other hand, evaporation from shallow-rooted tropical pasture falls during dry periods and is about half that from nearby forest.

For the selected FLUXNET sites, Fig. 2 shows comparisons between the monthly average modeled evaporation, observed evaporation renormalized so that the sum of the net outgoing latent and sensible heat fluxes is equal to the modeled available energy, and, for reference, the observed air temperature and rainfall. Table 2 provides an overview of the seasonality of observed evaporation and its relation to evaporative demand, the ratio of the annual averages of observed evaporation to evaporative demand, an overview of model performance when calculating the seasonal cycle of evaporation, and the ratio of the annual averages of modeled evaporation to evaporative demand. Among the most important deficiencies revealed in this comparison between modeled and observed evaporation are the following:

1. Evaporation is poorly represented if a fixed LAI is assumed in JULES at sites where the vegetation has a strong seasonal phenology (e.g., crops and deciduous trees) but representation is improved when the seasonal variations taken from FLUXNET are used.
2. The seasonality in modeled evaporation for tropical forest is too great in JULES, likely because the rooting depth used in the model is too shallow.
3. Frozen soils are not always well represented; JULES models transpiration when observations suggest it is still restricted by frozen soil.

b. Speed of dry down

The speed with which soils dry out after wet periods is an important aspect of the land surface influence on the atmosphere. The data from the Sahel (Gash et al. 1991), for example, showed water was stored over long time periods for vegetated areas of landscape, which can affect the meteorology of the region. Teuling et al. (2006) demonstrated that vegetated areas in the Sahel take longer to dry out than what many land surface models simulate, while Taylor and Clark (2001) showed that the speed of drying has an effect on the regional rainfall pattern.

Teuling et al. (2006) defined a parameter, the *e*-folding time of the evaporation, to represent the dry-down phenomenon. During dry periods, it is assumed that the available moisture at the land surface available to the atmosphere S (mm) is first rapidly depleted by drainage after a wet period but is then mainly depleted by the evaporation AE (mm day^{-1}). The water balance of the near-surface water store during evaporative dry down is therefore given at time t (days) by

$$\frac{dS}{dt} = -\mathrm{AE}. \tag{2}$$

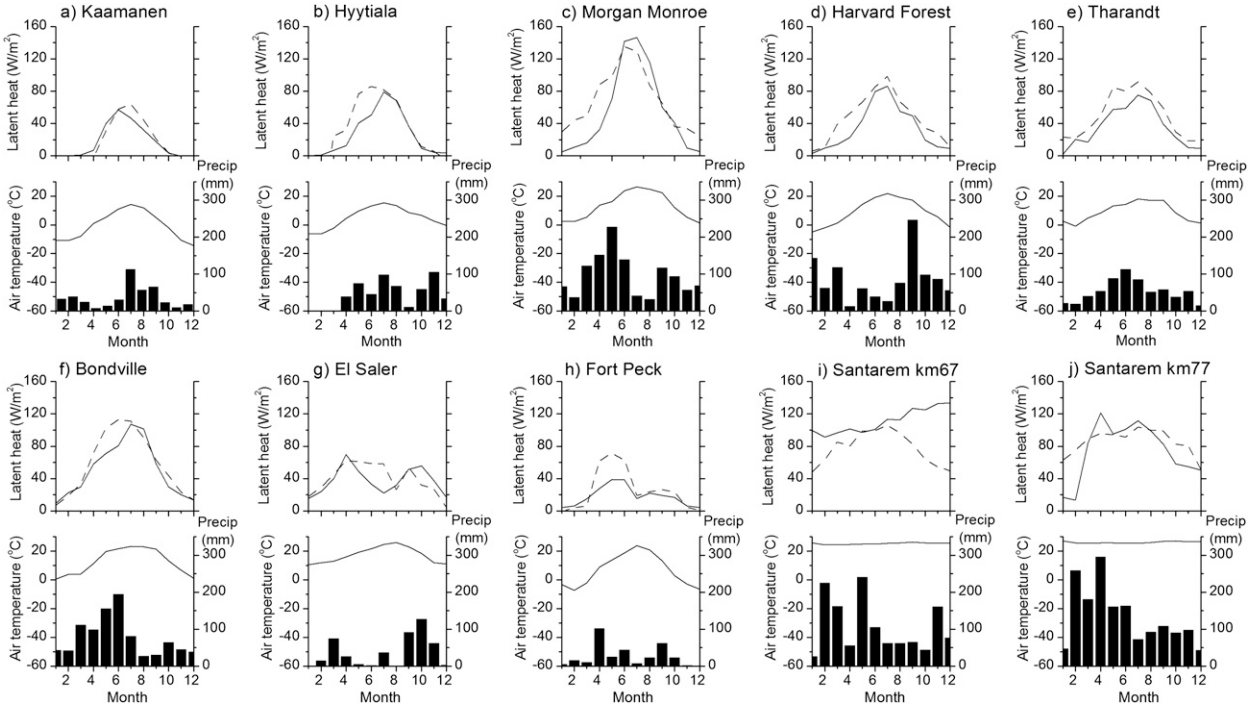

FIG. 2. Monthly-mean observed evaporation (E_{OB}, solid thick line) and modeled evaporation (E_{MOD}, solid thick broken line) air temperature (thin solid line), and rainfall (bar chart) for the following FLUXNET sites: (a) Kaamanen, (b) Hyytiälä, (c) Morgan Monroe, (d) Harvard Forest, (e) Tharandt, (f) Bondville, (g) El Saler, (h) Fort Peck, (i) Santarem km 67, and (j) Santarem km 77.

If after the first 24 h of drainage (when, it is assumed, the soil has reached field capacity) surface evaporation is assumed to be constrained and linearly related to the available moisture store and providing there is no more rain or drainage, evaporation changes with time as follows:

$$\mathrm{AE} = -\frac{S}{\tau},$$

where τ is the *e*-folding time of the surface in days. This equation can be solved with (2) as follows:

$$\mathrm{AE} = \mathrm{AE}_0 \exp\left(-\frac{t - t_0}{\tau}\right), \tag{3}$$

where AE_0 (mm day^{-1}) is the evaporation at time $t = t_0$. This model of evaporation assumes that evaporative demand remains constant. As demonstrated by Daly and Porporato (2006), the variations in potential evaporation do not strongly affect the slower time-scale variations of moisture availability. Consequently, in this analysis the *e*-folding time of the ratio observed evaporation to evaporative demand was used.

In practice, only 2 of the 10 selected FLUXNET sites—the two with Mediterranean climate; that is, El Saler and Fort Peck—had data for sufficiently long dry periods to identify the *e*-folding time of surface evaporation. Figure 3 shows that both the logarithm of the ratio between observed evaporation and evaporative demand and the ratio between modeled evaporation and evaporative demand have an approximately linear relationship with time. The linear relationship for observed evaporation at the El Saler site has an r^2 of 0.24 and corresponds to an *e*-folding time of 190 days, whereas Fort Peck has an r^2 of 0.93 and corresponds to an *e*-folding time of 16 days. Arguably, the El Saler site dries down more slowly because the site is populated by trees that can access water to greater depth through deeper roots than can the grassland at the more rapidly drying Fort Peck site. For modeled evaporation, the linear relationship at the El Saler site has an r^2 of 0.73 and corresponds to an *e*-folding time of 42 days (i.e., significantly shorter than observed), whereas Fort Peck has an r^2 of 0.85 and corresponds to an *e*-folding time of 13 days (i.e., roughly similar but slightly less than that observed).

c. *Hourly evaporation*

At time scales of less than a day, the surface and overlying atmosphere are not necessarily in equilibrium. The cloud cover can change, wind speeds can alter, and air can be brought into the area with different

TABLE 2. For each FLUXNET site, description of the seasonality of E_{OB} and its relation to evaporative demand, the ratio of the annual averages of E_{OB} to evaporative demand (E_{PT}), description of the seasonality of evaporation, the model performance, and ratio of the annual averages of E_{MOD} to E_{OB} scaled by the available energy with the RMSE in parentheses.

Site (climate)	Seasonality characteristics	Annual E_{OB}/E_{PT}	Model performance	Annual E_{OB}/E_{PT} (RMSE in W m^{-2})
KA (boreal)	Low evaporative demand and short growing season; E_{OB} follows E_{PT} in summer, but it is low when soil frozen in winter	0.94	E_{MOD} follows the seasonal cycle of the E_{OB}, although it is too low in winter and the increase in spring is too late	0.98 (6.5)
HY (boreal)	Seasonality dominated by frozen soil; E_{OB} low in winter and spring, but it reaches E_{PT} in late summer	0.79	E_{MOD} follows the seasonal cycle of E_{OB}, but it is too low in winter and too high in summer	1.35 (16.5)
MM (temperate)	E_{OB} reflects seasonal cycle in leaf area between May, but it follows E_{PT} in summer	0.74	E_{MOD} follows the seasonal cycle of E_{OB} well, although it increases too quickly in spring	1.25 (27.2)
HF (temperate)	E_{OB} low compared to E_{PT} in winter and into spring (no leaves), but it follows E_{PT} in summer	0.60	E_{MOD} follows the seasonal cycle of E_{OB} well, although it increases too quickly in spring	1.37 (15.6)
TH (temperate)	Observed evaporation follows evaporative demand, but low rainfall means E_{OB} always less than E_{PT} especially in winter	0.74	E_{MOD} follows the seasonal cycle of E_{OB}, al though it is too high in winter.	1.38 (15.2)
BV (temperate)	Seasonal cycle in E_{OB}, but it differs from E_{PT}; late rise in E_{OB} in spring and sharp fall in the autumn likely reflects cropping cycle	0.83	E_{MOD} follows the E_{OB} well, except in spring when it is too high	1.09 (10.4)
FP (Mediterranean)	Distinct Mediterranean seasonality; E_{OB} dips to a minimum in June when the rainfall low despite high E_{PT}	0.43	E_{MOD} follows the seasonal pattern of E_{OB} well, although it peaks too high in spring	1.44 (16.1)
ES (Mediterranean)	Precipitation low (~60 mm) with hot dry summer; E_{OB} peaks in spring and autumn but very low in the summer and winter	0.41 (reflects low summer E_{OB})	E_{MOD} follows the seasonal pattern of E_{OB}, but it reduces to early in the summer and too late in winter	0.93 (16.2)
S67 (humid tropics)	Little seasonality; selected year had little rain but E_{OB} drops only slightly compared to E_{PT}	0.85	E_{MOD} has an entirely different seasonal pattern to E_{OB}, with a high evaporation in summer and low in winter	0.77 (43.7)
S77 (humid tropics)	Little change in temperature, but E_{OB} drops with rainfall in summer–early winter; E_{OB} similar to E_{PT} after early spring rains	0.64	E_{MOD} follows the seasonal cycle of E_{OB}, but it has too high evaporation in winter	1.04 (26.3)

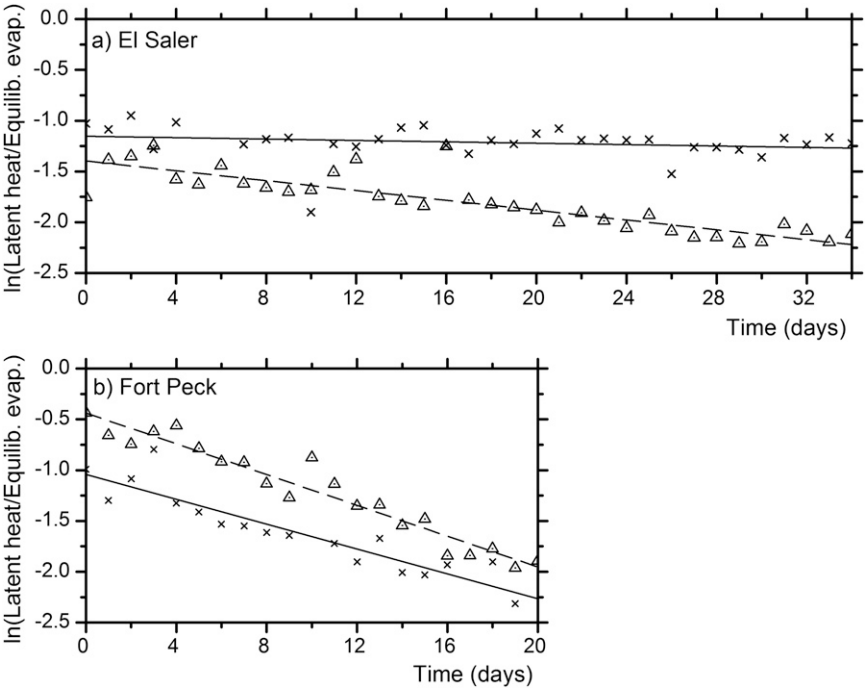

FIG. 3. Natural logarithm of the ratio of daily average E_{OB} to evaporative demand (solid line, crosses) and natural logarithm of the ratio of daily model-calculated evaporation to evaporative demand (dashed line, triangles) against day number during an extended dry period for (a) El Saler and (b) Fort Peck FLUXNET sites. The linear regression lines are also shown. The r^2 value for El Saler (Fort Peck) is 0.73 (0.85).

temperature and humidity. At this time scale, evaporative demand is better characterized by the Penman equation (Penman 1948). The Penman equation was designed for application at the daily time scale; however, in this study, it is applied each hour and takes the form

$$\lambda E_p = \frac{\Delta A_p + \rho c_p D(1 + 0.536.U)/250}{\Delta + \gamma}, \qquad (4)$$

where λE_p is the hourly average outgoing latent heat flux, D is the vapor pressure deficit, ρ is the density of air, c_p is the specific heat of air at constant pressure, and A_p is the energy available for evaporation for the selected hour [cf. A in Eq. (1)]. To impose consistency with FLUXNET observations and to compensate for possible mismeasurement in these observations, A_p is set equal to the modeled value of available energy in this analysis.

At hourly time scales, the effect of diurnal changes in plant control can become apparent through changes in the relationship between observed hourly evaporation and the hourly estimates of evaporative demand calculated using Eq. (4). An important finding of micrometeorological research (e.g., Shuttleworth 1989) is the evidence that evaporation tends to fall off relative to evaporative demand in the afternoon. This is an important feature in hot, semiarid regions where the increase in the air temperature as a response to a drop in evaporation has a strong effect on increasing the vapor pressure deficit and therefore the evaporative demand. Alternative explanations for the drop in actual evaporation are that the transpiring plants close their stomata in response to atmospheric demand in the form of the higher afternoon air temperature and vapor pressure deficit, or that plants respond to carbon accumulation and in arid regions increase their chances of survival by closing stomata to conserve water once they have reached the required daily carbon uptake. It is of interest to investigate whether stomatal closure is happening more generally at the FLUXNET sites and, in particular, whether the JULES model is simulating such closure if it does occur. Investigation was therefore made of the model's ability to reproduce any observed diurnal changes in the ratio of observed evaporation to evaporative demand as calculated by Eq. (4).

Short-term water stress was not observed in the FLUXNET data for 8 of the 10 sampled sites, and the diurnal cycle of observed evaporation tended to follow that of evaporative demand. However, during dry periods at Fort Peck and El Saler, the two Mediterranean sites, evidence of stomatal closure during the day was found. Figure 4 shows the daily variation in observed evaporation

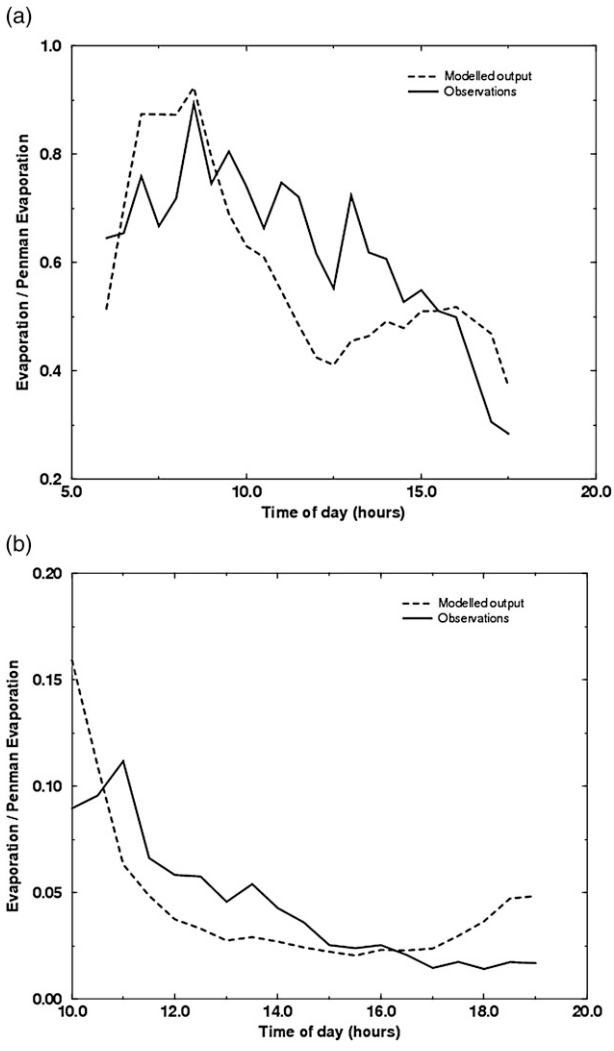

FIG. 4. Four-day average of diurnal variation in the ratio of E_{OB} to evaporative demand and natural logarithm of the ratio of model-calculated evaporation to evaporative demand against day number for (a) El Saler and (b) Fort Peck FLUXNET sites. Solid line represents observations and the dashed line represents the modelled output.

and evaporative demand averaged over four days at these two sites. At El Saler, observed evaporation falls progressively throughout the day relative to evaporative demand from a ratio of about 0.8 to about 0.5. At Fort Peck, the ratio of observed hourly evaporation to evaporative demand also falls progressively but more dramatically, by a factor of 10 through the day from a value of about 0.1 to about 0.01. Perhaps the less dramatic drop at the El Saler site reflects trees having better access to soil water through their deep roots.

At El Saler, the JULES model simulation of hourly evaporation is higher in the morning, drops in the afternoon, and then rises again in the evening unlike the observed evaporation, which drops gradually through the day. Modeled hourly evaporation for the Fort Peck site also drops in the morning, stays low through the day, and then rises again in the evening. Thus, the comparison between modeled and observed evaporation shows distinctly different diurnal variations for dry land surfaces at both sites. Modeled evaporation peaks in the morning and then falls quickly during the day, whereas observations show a steadier decline. To quantify whether any changes to the model had either improved or degraded this aspect of the evaporation character, the error in the hourly evaporation, averaged over the four days, was quantified. This can then be used for future reference. The root-mean-square error (RMSE) in the mean hourly evaporation ratio shown in Fig. 4 was 0.217 (dimensionless ratio) at El Saler and 0.614 (dimensionless ratio) at Fort Peck.

5. Conclusions

This study confirms the results of Stöckli and Vidale (2005), who demonstrated that offline simulations allow computationally inexpensive research and development of the land surface models in GCMs. The present study also shows that data from just 10 FLUXNET sites with high-quality, subdiurnal observations can be valuable when evaluating the performance of the land surface model physics that controls the partition of incoming radiant energy into evaporation, providing the selected sites sample with a sufficiently broad range of climate zones and plant functional types. However, a larger range of plant functional types might be required to evaluate the performance of the carbon processes in the model.

This study focused on investigating the JULES model's ability to describe essential evaporation-related features, specifically total annual evaporation, seasonal variations in evaporation, speed of drying after rainfall, and diurnal variations in evaporation rate. It did so by selecting a range of FLUXNET sites at which evaporation is affected by many different factors, including soil drying, plant stomatal control, the influence of soil freezing on soil hydraulics, and the effect of vegetation structure and cover on transpiration and interception loss. To make the evaluation, it was necessary to assume that the fractional mismeasurement of energy outgoing as latent and sensible heat in FLUXNET data is the same, on average.

The results reveal some deficiencies in the JULES model's ability to partition radiation as evaporation that merit further attention. The most important of these deficiencies being the following:

- In general, the JULES evaporation is higher than that observed;

- Using fixed annual leaf area in JULES means evaporation is poorly described at sites where vegetation has marked phenology (e.g., annual crops and deciduous trees);
- Evaporation tends to falls too quickly during extended dry periods. This is arguably a common feature in land surface models that assume universal properties for vegetation types where perennial dryland vegetation has adapted to survive long dry periods;
- The modeled seasonal dependence of tropical forest evaporation is too great, probably because the assumed rooting depth is too shallow;
- Frozen soils are not well represented by the model: in cold climates the model simulates evaporation when observations indicate that transpiration remains inhibited by frozen soil; and
- Modeled and observed evaporation have distinctly different diurnal variation for dry land surfaces. Observations show a steady decline during the day, whereas the model calculates high morning and evening evaporation with low evaporation between which may suggest soil hydraulic control is being overestimated.

Much progress has already been made in recent JULES development to address the shortcomings highlighted here. This series of tests of model description of evaporation at different time scales acts as a benchmark of the performance of JULES in its operational mode, and it will allow us to compare model performance following model changes with reference to the invaluable subdaily observations.

Acknowledgments. We gratefully acknowledge the FLUXNET PIs at all the sites from which data were taken for this study and the institutions and agencies that support data collection at these sites, including Dr. Laurila of the Finnish Meteorological Institute, Dr. Vesala of the University of Helsinki, Drs. Monroe and Dragoni of the Indiana University, Dr. Wofsy of Harvard University, Dr. Bernhofer of the IHM Technical University of Dresden, Dr. Meyers of NOAA/ARL, Dr. Sanz of the Fundación CEAM Parque Technológico, and Dr. Fitzgerald of the University of Albany. M. Pryor and G. P. Weedon were supported by the Joint DECC, Defra, and MoD Integrated Climate Programme by DECC/Defra (GA01101) and MoD (CBC/2B/0417_Annex C5).

REFERENCES

Baldocchi, D., and Coauthors, 2001: FLUXNET: A new tool to study the temporal and spatial variability of ecosystem-scale carbon dioxide, water vapor, and energy flux densities. *Bull. Amer. Meteor. Soc.,* **82,** 2415–2433.

Bates, B. C., Z. W. Kundzewicz, S. Wu, and J. P. Palutikof, Eds., 2008: Climate change and water. IPCC Tech. Paper 6, 214 pp.

Blyth, E. M., 2008: Modelling catchment scale evaporation—What are the errors? *Water Resources Research Progress,* L. N. Robinson, Ed., Nova Publishers, 297–310.

——, and Coauthors, 2006: JULES: A new community land surface model. *Global Change Newsletter,* No. 66, IGBP, Stockholm, Sweden, 9–11.

Cox, P. M., R. A. Betts, C. B. Bunton, R. L. H. Essery, P. R. Rowntree, and J. Smith, 1999: The impact of new land surface physics on the GCM sensitivity of climate and climate sensitivity. *Climate Dyn.,* **15,** 183–203.

Daly, E., and A. Porporato, 2006: Impact of hydroclimatic fluctuations on the soil water balance. *Water Resour. Res.,* **42,** W06401, doi:10.1029/2005WR004606.

De Bruin, H. A. R., 1983: A model for the Priestley-Taylor parameter α. *J. Climate Appl. Meteor.,* **22,** 572–578.

Finnigan, J. J., 2004: A re-evaluation of long-term flux measurement techniques. Part II: Coordinate systems. *Bound.-Layer Meteor.,* **113,** 1–41.

——, R. Clement, Y. Malhi, R. Leuning, and H. A. Cleugh, 2003: A re-evaluation of long-term flux measurement techniques. Part I: Averaging and coordinate rotation. *Bound.-Layer Meteor.,* **107,** 1–48.

Gash, J. H. C., and A. J. Dolman, 2003: Sonic anemometer (co)sine response and flux measurement: I. The potential for cosine error to affect flux measurements. *Agric. For. Meteor.,* **119,** 195–207.

——, J. S. Wallace, C. R. Lloyd, A. J. Dolman, M. V. K. Sivakumar, and C. Renard, 1991: Measurements of evaporation from fallow Sahelian savannah at the start of the dry season. *Quart. J. Roy. Meteor. Soc.,* **117,** 749–760.

Gerrits, A. M. J., H. H. G. Savenije, L. Hoffmann, and L. Pfister, 2007: New technique to measure forest floor interception? An application in a beech forest in Luxembourg. *Hydrol. Earth Syst. Sci.,* **11,** 695–701.

Goutorbe, J. P., and Coauthors, 1997: An overview of HAPEX-Sahel: A study in climate and desertification. *J. Hydrol.,* **188–189,** 4–17.

Guevara-Escobar, A., E. Gonzalez-Sosa, M. Ramos-Salinas, and G. D. Hernandez-Delgado, 2007: Experimental analysis of drainage and water storage of litter layers. *Hydrol. Earth Syst. Sci.,* **11,** 1703–1716.

Harding, R. J., S.-E. Gryning, S. Halldin, and C. R. Lloyd, 2001: Progress in understanding of land surface/atmosphere exchanges at high latitudes. *Theor. Appl. Climatol.,* **70,** 5–18.

Haverd, V., M. Cuntz, R. Leuning, and H. Keith, 2007: Air and biomass heat storage fluxes in a forest canopy: Calculation within a soil vegetation atmosphere transfer model. *Agric. For. Meteor.,* **147,** 125–139.

Lawrence, D. M., P. E. Thornton, K. W. Oleson, and G. B. Bonan, 2007: The partitioning of evapotranspiration into transpiration, soil evaporation, and canopy evaporation in a GCM: Impacts on land–atmosphere interactions. *J. Hydrometeor.,* **8,** 862–880.

Mauder, M., and Coauthors, 2007: The energy balance experiment EBEX-2000. Part II: Intercomparison of eddy-covariance sensors and post-field data processing methods. *Bound.-Layer Meteor.,* **123,** 29–54.

McNaughton, K. G., and T. W. Spriggs, 1989: An evaluation of the Priestley and Taylor equation and the complementary relationship using results from a mixed-layer model of the convective boundary layer. *Estimation of Areal Evapotranspiration,* IAHS Publication 177, 89–104.

Meyers, T., and S. E. Hollinger, 2004: An assessment of storage terms in the surface energy balance of maize and soybean. *Agric. For. Meteor.,* **125,** 105–115.

Nobre, C. A., J. H. C. Gash, J. M. Roberts, and R. L. Victoria, 1996: The conclusions from ABRACOS. *Amazonian Deforestation and Climate,* J. H. C. Gash et al., Eds., John Wiley & Sons, 577–595.

Oncley, S. P., and Coauthors, 2007: The Energy Balance Experiment EBEX-2000. Part I: Overview and energy balance. *Bound.-Layer Meteor.,* **123,** 1–28.

Penman, H. L., 1948: Natural evaporation from open water, bare soil and grass. *Proc. Roy. Soc. London,* **193A,** 120–145.

Priestley, C. H. B., and R. J. Taylor, 1972: On the assessment of surface heat flux and evaporation using large-scale parameters. *Mon. Wea. Rev.,* **100,** 81–92.

Sellers, P. J., W. J. Shuttleworth, J. L. Dorman, A. Dalcher, and J. M. Roberts, 1989: Calibrating the Simple Biosphere Model for Amazonian tropical forest using field and remote sensing data. Part I: Average calibration with field data. *J. Appl. Meteor.,* **28,** 727–759.

Shuttleworth, W. J., 1989: Micrometeorology of temperate and tropical forest. *Philos. Trans. Roy. Soc. London,* **324B,** 299–334.

Stewart, J. B., 1977: Evaporation from the wet canopy of a pine forest. *Water Resour. Res.,* **13,** 915–921.

Stöckli, R., and P. L. Vidale, 2005: Modelling diurnal to seasonal water and heat exchanges at European FLUXNET sites. *Theor. Appl. Climatol.,* **80,** 229–243.

——, and Coauthors, 2008: Use of FLUXNET in the Community Land Model development. *J. Geophys. Res.,* **113,** G01025, doi:10.1029/2007JG000562.

Taylor, C. M., and D. B. Clark, 2001: The diurnal cycle and African easterly waves: A land surface perspective. *Quart. J. Roy. Meteor. Soc.,* **127,** 845–867.

Teuling, A. J., S. I. Seneviratne, C. Williams, and P. A. Troch, 2006: Observed timescales of evaporatranspiration response to soil moisture. *Geophys. Res. Lett.,* **33,** L23403, doi:10.1029/2006GL028178.

Twine, E., and Coauthors, 2000: Correcting eddy-covariance flux underestimates over a grassland. *Agric. For. Meteor.,* **103,** 279–300.

van der Molen, M. K., J. H. C. Gash, and J. A. Elbers, 2004: Sonic anemometer (co)sine response and flux measurement: II. The effect of introducing an angle of attack dependent calibration. *Agric. For. Meteor.,* **122,** 95–109.

Wilson, K., and Coauthors, 2002: Energy balance closure at FLUXNET sites. *Agric. For. Meteor.,* **113,** 223–243.